

Dynamical Simulations of Supernovae Collapse and Nuclear Collisions via the Test Particle Method - Similarities and Differences

Wolfgang Bauer^{1,a}

¹ Department of Physics and Astronomy and
National Superconducting Cyclotron Laboratory
Michigan State University
East Lansing, MI 48824-2320, USA

Abstract. Test particle methods have been applied very successfully to the numerical simulation of heavy ion reactions at intermediate and high beam energies. Here we will show that the same techniques can be used successfully to simulate the dynamics of the collapse of type II supernovae precursors. We will focus special attention on the effects of collective angular momentum on the resulting supernova dynamics.

Keywords: Heavy ion collision, test particle simulation, particle spectra, flow, interferometry, supernova, type II, precursor, phase space dynamics, angular momentum.

PACS: 24.10.-i, 24.10.Lx, 25.70.-z, 25.75.-q, 26.50.+x, 97.60.Bw

1. Nuclear Dynamics

Wong [1] showed in 1982 that it is possible to approximate the quantum nuclear many body problem solution on the mean field level (TDHF) via a semiclassical approach based on test particles formulation. In this method, one follows the initially (completely or partially) occupied cells in the 6-dimensional phase space as a function of time. At about the same time, Cugnon and collaborators [2, 3] implemented ideas of intra-nuclear cascades, i.e. an approximation without a nuclear mean field, in which two-body collisions exclusively determine the nuclear dynamics. Bertsch and collaborators [4–7] and then several other groups around the World [8–15] combined both ideas to produce a solution of the nuclear transport equation

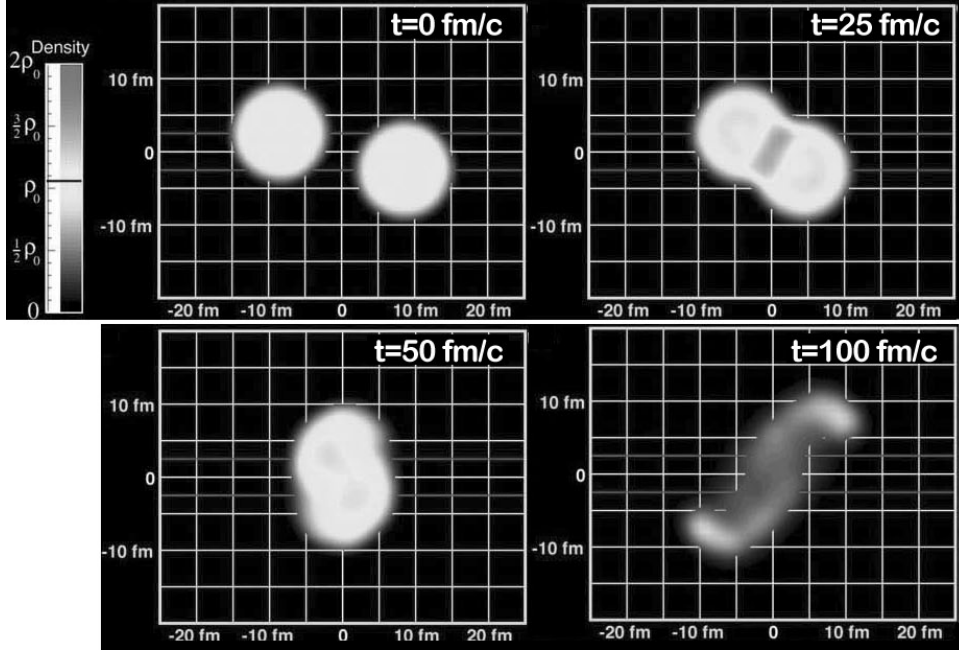


Fig. 1. Time evolution of a typical heavy ion collision at intermediate energy. Shown here is the baryon density in the reaction plane for a 60 A MeV Au + Au collision at an impact parameter of 5 fm. The 4 frames shown were taken at times 0, 25, 50, and 100 fm/c. [19].

(Boltzmann-Uehling-Uhlenbeck, BUU, also VUU, BN, ...),

$$\begin{aligned}
\frac{\partial}{\partial t} f(\vec{r}, \vec{p}, t) &+ \frac{\vec{p}}{m} \vec{\nabla}_r f(\vec{r}, \vec{p}, t) - \vec{\nabla}_r U \vec{\nabla}_p f(\vec{r}, \vec{p}, t) \\
&= \frac{g}{2\pi^3 m^2} \int d^3 q_1' d^3 q_2 d^3 q_2' \\
&\delta \left(\frac{1}{2m} (p^2 + q_2^2 - q_1'^2 - q_2'^2) \right) \cdot \delta^3(\vec{p} + \vec{q}_2 - \vec{q}_1' - \vec{q}_2') \cdot \frac{d\sigma}{d\Omega} \\
&\cdot \left\{ f(\vec{r}, \vec{q}_1', t) f(\vec{r}, \vec{q}_2', t) \left(1 - f(\vec{r}, \vec{p}, t) \right) \left(1 - f(\vec{r}, \vec{q}_2, t) \right) \right. \\
&\quad \left. - f(\vec{r}, \vec{p}, t) f(\vec{r}, \vec{q}_2, t) \left(1 - f(\vec{r}, \vec{q}_1', t) \right) \left(1 - f(\vec{r}, \vec{q}_2', t) \right) \right\}.
\end{aligned} \tag{1}$$

in the test particle approximation. In this approximation the solution of the above integro-differential equation can be reduced to the simultaneous solution of \mathcal{N} cou-

pled first-order differential equations in time:

$$\begin{aligned} \frac{d}{dt}\vec{p}_i &= -\vec{\nabla}U(\vec{r}_i) + \sum_{j \neq i} \frac{q_i q_j}{(\vec{r}_i - \vec{r}_j)^2} + \mathcal{C}(\vec{p}_i), \\ \frac{d}{dt}\vec{r}_i &= \frac{\vec{p}_i}{\sqrt{m_i^2 + p_i^2}}, \\ i &= 1, \dots, (A_t + A_p)\mathcal{N}, \end{aligned} \quad (2)$$

where A_t and A_p are the target and projectile masses, respectively, and \mathcal{N} is the number of test particles per nucleon (usually taken > 100 to reduce artificially generated numerical fluctuations).

The term $\mathcal{C}(\vec{p}_i)$ represents the solution of the collision integral via an intranuclear cascade for the test particles. The test particle collisions respect the Pauli exclusion principle due to the presence of the factors $(1 - f)$, which are numerically implemented via a Monte Carlo rejection method. In our particular numerical realization the values of $f(\vec{r}, \vec{p}, t)$ are stored in a six-dimensional lattice so that the computation of the factors $(1 - f(\vec{r}, \vec{p}, t))$ only requires the call of 2^6 lattice elements for a six-dimensional interpolation [18].

Fig. 1 shows a typical time evolution of a heavy ion collision that results from this approach. We have grown confident that this simulation captures the essentials of the nuclear dynamics, because BUU-type approaches have been incredibly successful in reproducing all kinds of experimental observables, such as the emission spectra of protons and neutrons, the coalescence of small fragments, the nuclear collective flow, and production of secondary particles (photons, pions, kaons, ...), and even Hanbury-Brown-Twiss type interferometry [16, 17].

2. Type II Supernovae

We currently distinguish two types of supernova events. In type I supernovae, a white dwarf exceeds its Chandrasekhar Mass ($\sim 1.4 M_\odot$) due to accretion and collapses. We want to focus here on type II supernova events associated with the violent death of stars at the end of their thermonuclear fuel cycle. These are powered by the gravitational energy released during a star's late stage iron core collapse, caused by instabilities due to electron capture ($p + e^- \rightarrow n + \nu_e$) or photodisintegration (${}^{56}\text{Fe} + \gamma \rightarrow 14 {}^4\text{He} + 4n$, ${}^4\text{He} + \gamma \rightarrow 2p + 2n$). The first process dominates for precursor mass ranges between 10 and 20 solar masses ZAMS (= zero age main sequence; mass of the star at the beginning of its evolution), and the second for masses in the range between 20 and 40 solar masses ZAMS.

The numerical study of supernova explosions has been a mainstay of astrophysics for the last few decades, relying in hydrodynamical codes that run on the largest available computer systems. It has turned out that these hydro simulations are of incredible complexity, due to the rapidly changing length scales during the collapse phase, due to the changing viscosity as a function of time, due to the relatively long evolution that one has to simulate (only a few milliseconds in real time,

but a very large number of time steps in the computer), and due to the coupling to the neutrino Boltzmann transport. In particular the modeling of the neutrinos has proven to be difficult, and the outcome of the simulation (explosion or stalling of the shock) has turned out to be very sensitive on the details of this part of the calculation.

3. Test Particle Approach for Supernova Dynamics

Can the test particle approach discussed in section 1 be utilized for the dynamics of core collapse simulations of type II supernovae? The answer is yes. We can re-cast the hydrodynamical time evolution equations for the iron core matter in terms of test particle equations. The first question, however, is what a test particle is to represent in physical space. If we utilize a total number of N_{tp} test particles in our simulations, and we consider a typical iron core mass of order λM_\odot , then the mass of each test particle, m_{tp} , is given by $\lambda M_\odot / N_{tp}$. Using 10^7 test particles, for example, we obtain typical test particle masses of 1/10 of that of Earth. The resulting test particle time evolution equations are:

$$\begin{aligned} \frac{d}{dt} \vec{p}_j &= -\vec{\nabla} U_{\text{EoS},e^-}(\vec{r}_j) + \vec{F}_{G,j}(\vec{r}_1, \dots, \vec{r}_{N_{tp}}) + \mathcal{C}(\vec{p}_j) + \mathcal{C}_\nu(\vec{p}_j) \\ \frac{d}{dt} \vec{r}_j &= \frac{\vec{p}_j}{\sqrt{m_{tp}^2 + p_j^2}} \\ j &= 1, \dots, N_{tp}, \end{aligned} \quad (3)$$

where $\vec{F}_{G,j}$ denotes the force on particle j due to gravity and $\vec{F}_{EOS,j}$ the force due to the equation of state. Gravity is modeled using the Newtonian monopole approximation:

$$\vec{F}_{G,j} = -G \frac{m_{tp}^2 \#\{i \in \{1, \dots, N_{tp}\} : |\vec{r}_i| < |\vec{r}_j|\}}{|\vec{r}_j|^3} \vec{r}_j. \quad (4)$$

This approximation is obviously only appropriate as long as the deviations from spherical symmetry are sufficiently small.

As a realistic EOS, $\vec{F}_{EOS,j}$, for core collapse conditions we used a combination of the nuclear EOS by Lattimer & Swesty [20] and the Helmholtz EOS by Timmes (which is an EOS for the electron/positron gas) [21]. The former is used for $\rho \geq 10^{11} \text{g/cm}^3$, the latter for $\rho < 10^{11} \text{g/cm}^3$ where the nuclear contribution to the pressure is negligible.

The Term $\mathcal{C}(\vec{p}_j)$ represents again the effects of the test-particle cascade, i.e. two-body scattering events between test particles. During the initial phase of the collapse the velocities scale with the radial distance, and the effects of this two-body scattering term is small, however, in the late phases, and in particular during the shock formation, it becomes dominant.

The term $\mathcal{C}_\nu(\vec{p}_j)$ represent the effects of the scattering of neutrinos off the baryonic test particles. The corresponding time evolution equations for the neutrinos have a source term originating from two-particle collisions and form coupled equations with the above baryon time evolution equations. This part of the dynamics is not implemented as of yet and will be work to be accomplished in the near future. However, we anticipate that the formalism is in complete analogy to the implementation of coupled transport equations for baryons, resonances, and mesons in relativistic heavy ion collisions [14].

4. First Results

In an initial implementation of our ideas, we have concentrated on investigating the effects of total angular momentum, i.e. the rotation of the precursor star, on the collapse dynamics [22, 23]. Stellar evolution calculations for a rotating progenitor done by Heger [24] indicate that it is a very good approximation to assume that the inner core (initially) rotates like a rigid body. Therefore we used a constant initial angular velocity ω_0 .

$N_{tp} = 10^6$ test particles, the grid parameters $N_r = 110$, $N_{\cos\theta} = 100$, and a background density $\rho_{min} = 1.3 \times 10^{11} \text{g/cm}^3$ were applied in all runs of the series. Fig. 2 shows the density profiles of three different runs with different values of the initial angular velocity (70, 160, and 220 s^{-1} , from left to right). This corresponds to a ratio of rotational to gravitational energy of 1.3%, 6.8%, and 13%, respectively. While the bounce times are relatively insensitive to this parameter, the maximum central density reached is strongly dependent on it. We reach $\rho_{max} = 2.35\rho_0$ for the low angular momentum run, and values of $0.56\rho_0$ and $0.21\rho_0$ for the high angular momentum runs.

5. Conclusions

Test particle methods have been applied very successfully to the numerical simulation of heavy ion reactions at intermediate and high beam energies. Here we have shown that the same techniques can be used successfully to simulate the dynamics of the collapse of type II supernovae precursors. While neutrino transport is not fully implemented into our program, it seems clear that approaches based on test particle methods are excellent candidates to provide a fully 6-dimensional phase space simulation of the supernovae collapse and subsequent explosion, incorporating in particular the effects of collective angular momentum.

Acknowledgements

This research was supported by NSF grants PHY-0070818 and INT-9981342, as well as by an A. v. Humboldt U.S. Distinguished Senior Scientist award.

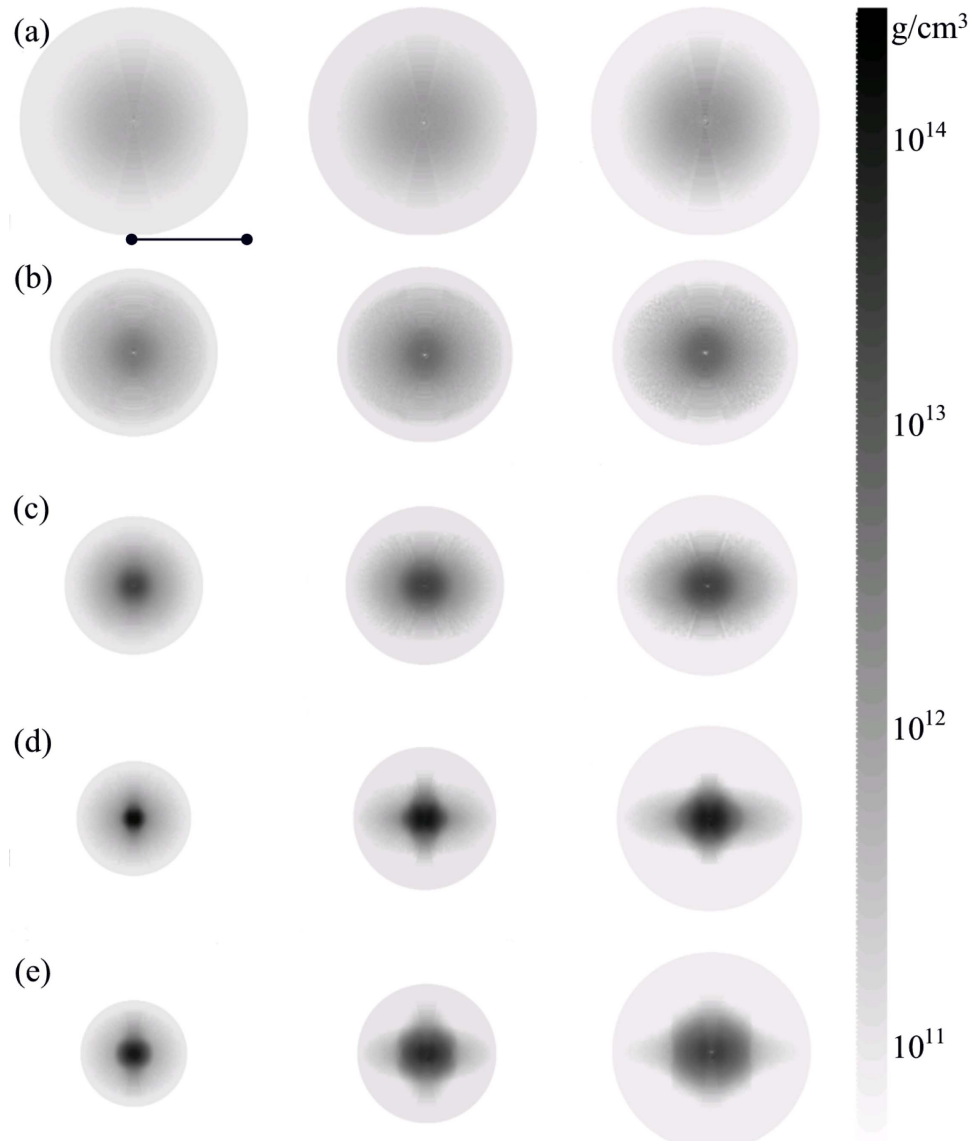


Fig. 2. Mass density in a slice in the x - z -plane at (a) onset of simulation, (b) after 2 ms, (c) 3 ms, (d) core bounce, (e) shortly after core bounce. All plots have the same radius scale (~ 120 km) indicated by the black line in the top left. From left to right, the initial angular velocities used in the simulation runs were 70, 160, and 220 s^{-1} .

Notes

- a. E-mail: bauer@pa.msu.edu
Home Page: <http://www.pa.msu.edu/~bauer/>

References

1. C.Y. Wong, *Phys. Rev. C* **25** (1982) 1460.
2. J. Cugnon, T. Mizutani, and J. Vandermeulen, *Nucl. Phys. A* **352** (1981) 505.
3. J. Cugnon, D. Kinet, and J. Vandermeulen, *Nucl. Phys. A* **379** (1982), 553.
4. G.F. Bertsch, H. Kruse, and S. Das Gupta, *Phys. Rev. C* **29** (1984) 673.
5. W. Bauer, G.F. Bertsch, W. Cassing, U. and Mosel, *Phys. Rev. C* **34** (1986) 2127.
6. G.F. Bertsch and S. Das Gupta, *Phys. Rep.* **160** (1988) 189.
7. P. Danielewicz and G.F. Bertsch, *Nucl. Phys. A* **533** (1991) 712.
8. H. Kruse et al., *Phys. Rev. Lett.* **54** (1985) 289.
9. H. Stöcker and W. Greiner, *Phys. Rep.* **137** (1986) 277.
10. J. Cugnon and M.C. Lemaire, *Nucl. Phys. A* **489** (1988) 781.
11. P. Schuck et al., *Prog. Part. Nucl. Phys.* **22** (1989) 181.
12. W. Cassing and U. Mosel, *Prog. Part. Nucl. Phys.* **25** (1990) 235.
13. B.A. Li and W. Bauer, *Phys. Lett.* **B254** (1991) 335.
14. S.J. Wang et al., *Ann. Phys. (N.Y.)* **209** (1991) 251.
15. A. Ono et al., *Prog. of Theor. Phys.* **87** (1992) 1185.
16. W. Bauer, C.K. Gelbke, and S. Pratt, *Annu. Rev. Nucl. Part. Sci.* **42** (1992) 77.
17. W. Bauer, *Prog. in Part. and Nucl. Phys.* **30** (1993) 45.
18. W. Bauer, *Phys. Rev. Lett.* **61** (1988) 2534.
19. A color version of this figure is on the back cover of the proceedings of the 18th Winter Workshop on Nuclear Dynamics.
20. J. Lattimer, and F. Swesty, *Nucl. Phys. A*, **535** (1991) 331; Equation of state version 2.7 (ls eos v2.7), <http://www.ess.sunysb.edu/dswesty/lseos.html>.
21. F. Timmes, and F. Swesty, *Astrophys. J. Suppl. S.* **126** (2000) 501; <http://flash.uchicago.edu/fxt/eos.shtml>.
22. T. Bollenbach, M.S. Thesis, Michigan State University (2002).
23. T. Bollenbach and W. Bauer, in “Exotic Clustering”, edited by S. Costa, A. Insolia, and C. Tùve, American Institute of Physics Conference Proceedings, Volume 644 (Melville, New York, 2002), p. 219-232.
24. A. Heger, N. Langer, and S. Woosley, *Astrophys. J.*, **528** (2000) 368.